MORPHOLOGICAL CHANGES DURING OXIDATION OF A SINGLE CHAR PARTICLE

Matteo d'Amore[^], Leonardo Tognotti[*], and Adel F. Sarofim[o]

[^]University of Salerno, Chemical and Food Engineering Dept., Italy

[*]University of Pisa, Chemical Engineering Department, Italy

[o]Massachusetts Institute of Technology, Chemical Engineering Dept. Cambridge, MA 02139 (U.S.A.)

Keywords: char oxidation; morphology; electrodynamic balance.

ABSTRACT

The evolution of pore size distribution during the oxidation of single Spherocarb char particles has been measured under chemical controlled conditions. Electrodynamically levitated particles were heated to reaction temperature using a laser and the weight and size changes monitored. The laser heating was interruypted at selected conversions and the CO_2 adsorption determined at ambient conditions. As reaction proceeds, particles are found to shrink, the macropore volume decreases in proportion to the total particle volume, maintaining a constant macroporosity. The micropore volume, however, decreases with increasing conversion whereas the normalized pore size distribution remains unchanged, suggesting that the densification of the microporous volume which leads to particle shrinkage results from pore elimination. At the same time the mesopore volume increases with increasing conversion indicating that the mesopores play a dominant role in the char reaction.

1. INTRODUCTION

The reaction rate of carbon burning under chemical kinetic or internal diffusion controlled regime is strongly affected by the pore structure, which governs the extent of penetration of the reacting gases and, through the porosity evolution with conversion, the total amount of surface available for reaction (Gavalas, 1980; Mohanty et al., 1982; Reyes and Jensen, 1986).

The problem of evaluating the variation of combustion rates with conversion is usually reduced to the purely topological problem of establishing the relationship between accessible surface area and porosity as this latter changes. In the above referenced theoretical studies the assumption is made either that the reactivity is constant over the entire surface or restricted to the non microporous area (Gavalas, 1980). Accessibility to the microporous area may be restricted due to hindered diffusion in pores having dimensions approaching that of the reacting molecules and reactivities may vary due to either graphitization of surfaces or non-uniform distribution of catalysts. For this reason it is

desirable to experimentally determine the evolution of pore structure with increasing carbon conversion.

Whatever the experimental technique used, the possible occurrence of phenomena like shrinkage (Hurt et al., 1988) or fragmentation by percolation (Bar-ziv et al., 1989; Kerstein and Niksa, 1985), complicates the analysis of data to obtain basic information on porosity and surface area. Moreover, the experimental apparatuses currently used for reactivity measurements and the porosimetry techniques presently available, even when used on small amounts of samples, yield average information, since they integrate the results over the entire number of particles used. All these uncertainties result in tremendous data scattering (up to four orders of magnitude at a given temperature) when general correlations for intrinsic reactivity of coal chars are proposed (Smith, 1982).

In this study, the changes with conversion in morphology of a carbon char in the temperature range 500-1200 K are followed by using an electrodynamic balance (EDB) (Spjut et al., 1985; Dudek, 1988; Bar-ziv et al., 1989). This device allows one to measure in situ, over temperature range wider than in other apparatuses, mass, diameter, density, surface area, rate of reaction and temperature for a single, suspended submillimeter particle. By following with the EDB the changes in the char as it reacts, it is possible to study the influence of the porous texture on the reaction behavior and shed some light on the contribution by micropores to the reaction in the chemical kinetic controlled regime.

The pore sizes will be broken down into three classes: micropores (diameters between 0.8 and 3 nm), mesopores (3 <d < 20 nm), and macropores (20 nm < d). The micropores will be determined by CO_2 gas adsorption and a significant part of the results and discussions in this paper will be devoted to the interpretation of adsorption data to obtain the finer pore structure. The macropores are traditionally obtained by mercury intrusion porosimetry, although precautions must be taken to separate the contribution of interparticle voids from those of the larger macropores (Bellezza, 1985). In this study the result of Hurt et al. (1988) that the macropore volume is constant during reaction in the kinetic controlled regime will be utilized. This result was based on the observation that all macrofeatures of a particle were conserved during reaction in a chemical controlled regime and that the changes in diameters of macropores, down to the limit of resolution of 100 nm on the electromicrographs, were proportional to the change in the particle diameter. The mesopores are traditionally measured by capillary condensation with the results being somewhat dependent on the method of interpretation of the adsorption-desorption isotherms. In this study the mesopores will be determined from a volume balance utilizing the special capability of the EDB for measuring the density of a single particle.

2. EXPERIMENTAL

2.1 Apparatuses

Electrodynamic Thermogravimetric Apparatus

The electrodynamic chamber consists of three electrodes in an hyperboloidal configuration, the theory of which is described by

Wuerker et al. (1959), Davis and Ray (1980), Philip (1981) and Spjut (1985). A schematic view of the electrodynamic balance is shown in Fig. 1. The chamber creates a dynamic electric field capable of suspending a single, charged particle with a characteristic size less than 250 μm in the present configuration. The AC or ring electrode provides lateral stability to the particle through an imposed AC field oscillating sinusoidally ±2000 volts at 100 Hz. The DC top and bottom electrodes provide vertical stability by balancing the gravitational force, thus stably suspending the charged particle in the chamber. A position control system can be used which automatically adjusts the electric field to keep the particle at the chamber center. An optical microscope is used for viewing the particle and for manual control of the particle position. The microscope allows the measurement of the particle diameter to ±5 μm. A 20 W CO_2 laser is used to heat the suspended particle and a two color infrared (2 and 4 μm) pyrometry is used for temperature measurements. A gas flow system allows one to react a particle in various gaseous enviroments. Additional details on the experimental apparatus and procedure can be found in Spjut et al. (1985), Bar-ziv et al.(1989), Dudek et al. (1988).

Porosimetry

The pore size distribution of the char was measured by means of a Carlo Erba Sorptomatic 1800 static-volumetric apparatus, using N_2 at 77 K or CO_2 at 195 and 298 K as adsorption gases, and a high pressure mercury porosimeter model Carlo Erba 2000. The EDB was used as a gravimetric apparatus for CO_2 adsorption measurements on single "Spherocarb" particles at 298 K.

2.2 Char properties

The model char used in this work was "Spherocarb", a spherical microporous carbon from Analabs Inc.. The 60/80 mesh commercial fraction has been used in several previous studies (Waters et al., 1988, Dudek et al., 1988, D'Amore et al., 1988, Hurt et al., 1988) because of its high degree of uniformity and sphericity. Furthermore, the low ash content of the particles minimizes the effects of catalytic impurities, while the limited amount of volatile matter precludes the complicating effects of devolatilization on the burning behaviour. The gross physical properties and the chemical analysis of the material are reported in the following section.

Size	180-240 μm
Particle density	0.63 gcm^{-3}
True density	2.10 gcm^{-3}
BET surface area	963 m^2g^{-1}
DR surface area	965 m^2g^{-1}
Total surface area	1025.6 m^2g^{-1}
Carbon content (weight basis, %)	96.9
Oxygen	2.4
Hydrogen	0.7

The BET area was obtained by analysing the N_2 adsorption isotherm at 77 K. Analysis of the CO_2 adsorption data at 195 and at 298 K by the Dubinin-Raduskevitch equation gave the DR area. The total surface area includes those of the micro-, meso-, and macro-pores. The good

agreement between the BET and the DR surface areas obtained in this case is somehow unexpected. Capillary condensation of the adsorption gases in the microporosity should be misinterpreted by Bet theory, which in this case would overestimate the sample surface area. On the other hand, indications have been given in the past that N_2 at 77 K hardly reaches the whole microporosity of chars. These counterbalancing effects could lead to the agreement above outlined.

Figure 2 shows the cumulative pore size distribution of the "Spherocarb" on a volume basis. The distribution has been obtained by joining distribution curves from gas adsorption together with results of high pressure mercury porosimetry (Dubinin, 1966; Spitzer et al., 1976). The method of Medek (1977) has been used to determine the size distribution of the micropores. Size distribution of mesopores has been obtained from adsorption data according to the method of Dollimore and Heal (1970). Mercury porosimetry has been used to determine the size distribution of macropores.

2.3 Experimental procedure with EDB

After capture in the EDB each particle was weighed by the technique described in detail elsewhere (D'Amore et al., 1988), and its diameter, density, porosity (D'Amore et al. 1988), surface area (Dudek et al. 1988) measured. The concentration of the gases flowing through the EDB was selected to include 5, 21 or 100% O_2 in N_2 or chromatographic-grade CO_2. The particle was heated by the $^2CO_2$ laser to the desired temperature which was measured by the two color optical pyrometry and continuously recorded. A semicontinuous reaction technique was utilized arresting the reaction by turning the laser off, and measuring at various conversions the physical parameters of the particle.

3. RESULTS

3.1 Microporosity

Theory

The adsorption data have been interpreted using the BET equation in the linear form:

$$\frac{p/p_s}{s(1-p/p_s)} = \frac{1}{s_m c} + \frac{c-1}{s_m c}\,(p/p_s) \qquad (1)$$

where s and s_m are the number of moles of gas adsorbed at relative pressure p/p_s and in a complete monolayer, per unit of sample mass, respectively.

For chars with a high fraction of microporosity, the low- and medium-pressure parts of isotherms are analysed using the Dubinin and Astakhov equation (Dubinin and Astakhov, 1971):

$$\theta = \frac{w}{w_{ts}} = \exp\,[-(A/E)]^h \qquad (2)$$

where w/w_{ts} is the ratio of the micropore volume w filled at pressure p/p_s to the total micropore volume w_{ts}, i.e. the degree of filling of micropores θ; E is the characteristic free energy of adsorption; A is the differential molar work of adsorption and is given by:

$$A = RT \ln(p_s/p) \qquad (3)$$

When w and w_{ts} are expressed in terms of moles of adsorbate s and s_{ts}, respectively, eq. (2) and (3) give:

$$\ln s - \ln s_{ts} = - (RT/E)^h [\ln (p_s/p)]^h \qquad (4)$$

For h=2 eq. (4) reduces to Dubinin-Raduskevitch equation (DR).

According to Medek's analysis (1977) the equation for the differential micropore size distribution is given by:

$$\frac{d\theta}{dr_e} = \frac{dw}{w_{ts} dr_e} = 3h\,(k/E)^h\, r_e^{-(3h+1)} \exp[-(k/E)^h\, r_e^{-3h}] \qquad (5)$$

where θ is the degree of filling of micropores, r_e the pore radius, k, evaluated according to Dubinin's affinity postulate, is equal to $7.51\ 10^{-25}$ cal m^{-3} $mole^{-1}$.

Evolution of "Spherocarb" morphology with reaction

By taking advantage of the special features of the electrodynamic balance, changes in physical characteristics of single "Sperocarb" particles with reaction have been followed.

The volume of micropores w_{ts} of single "Spherocarb" particles have been evaluated from the CO_2 adsorption isotherms at 298 K obtained in an EDB by the use of the DR equation. A complete description of the technique is given by Dudek et al. (1988). These volumes can be related to the surface areas of the micropores (Lamond and Marsh, 1964; Gan et al., 1972; Rand, 1974; Marsh et al., 1975). The char pores volumes are here reported (Figure 3) per unit mass of the particle being measured. In Figure 3, w_{ts} is reported versus fractional conversion f defined as the weight loss divided by the initial mass of carbon, for eight separate single particle "Spherocarb" oxidations. Five of the runs have been performed in oxygen, two in CO_2 and one in air. The reaction temperatures are in the range 750-830 K for reactions in oxygen and 1200-1250 K for reactions in CO_2. The initial specific volume of the micropores vary from 0.203 to 0.276 $cm^3\ g^{-1}$ with the average being 0.237 $cm^3\ g^{-1}$. These specific volumes can be compared to a value of 0.237 $cm^3\ g^{-1}$ obtained on a 0.294 g sample of "Spherocarb" (about 100,000 particles!) by Hurt et al (1988) in a conventional gravimetric apparatus. The specific volumes of the micropores for the 0.294 g sample at conversions of f=0 and f=0.65 for an oxidation run with air are also in Figure 3.

Adsorption can give, in addition to the total microporosities volumes, the pore size distribution by the use of eq. (5). Normalized distributions for fractional conversions f of 0.14, 0.23

and 0.52 for a single particle reacting in air at 770 K are compared in Figure 4 with the distributions for the unreacted char. Although the total microporous volume decreases, the fractional distribution of the residual pores is remarkably constant. This is consistent with the micropore elimination model of Hurt et al., (1988), which was presented with an alternative pore shrinkage model to explain the observation of shrinkage of particles when chemical kinetics are controlling.

3.2 Meso- and macro-porosities

The meso- and macro-porosities are obtained by volume balances on the single particle using measurements of the weight and volume of the particle to obtain total porosity.

Figure 5 shows the single particle porosity ϵ as a function of conversion for the same separate "Spherocarb" oxidations. The porosity values have been obtained from the particle densities by the relation:

$$\epsilon = (1 - \rho / \rho_t) \qquad (6)$$

where ρ is the density of a "Spherocarb" particle at a given conversion and ρ_t is the "Spherocarb" true density. Density measurements were performed discretely using the aerodynamic drag force technique (D'Amore et al., 1988). Initial porosities ranged from 0.56 to 0.68. Although conventional theory would predict particle porosity to increase linearly with conversion under kinetically controlled conditions (zone I) up to ϵ=1, the figure shows that the linearity holds up to a conversion of only 40-50%. A sort of plateau is then approached, consistent with the shrinkage-densification model proposed by Hurt et al. (1988) for chars undergoing regime I or kinetically controlled oxidation.

A particle shrinkage factor Σ has been defined as the ratio of the particle volume V to the initial volume V_0. The Σ values for the eight runs above have been reported in Fig. 6 as a function of conversion. The straight solid line in the figure represents a conventional shrinking, constant density, particle model, while the line at Σ=1 is representative of a purely internal reaction without shrinkage. The data indicates that the extent of "Spherocarb" shrinkage is not a function of temperature, or reacting gas, but only a function of conversion.

The data on total porosity and microporosity obtained in the EDB for a single particle allow one to evaluate the meso- and macropore volume of the particle at a given conversion. This can be done by a volume balance, given by the relation:

$$W = (1/\rho - 1/\rho_t - w_{ts}) (1-f) \qquad (7)$$

where W is the volume of the meso- plus macro-pores per unit initial mass. The results of such an analysis are reported in Fig. 7. In the figure, W has been normalized for each run with the initial value W_0, to account for the different characteristics of the single particles tested. In spite of the large differences in the initial porosity of the single particles (D'Amore et al., 1988), and in the

experimental conditions, clustering of the data points about one curve indicate that the particles all exhibit the same behavior: meso- plus macro-porosity increases with reaction, reaches a maximum at about f=0.3 and eventually decreases to zero at f=1, when the solid is consumed.

The meso- plus macro-pore volume fractions can be separated by utilization of the results of Hurt et al. (1988). Based on electronmicrographs studies of particles reacted to different fractional conversions, visible macropores (diameters greather than 100 nm) were found to have a constant volume fraction as particles shrank during conversion. Utilizing this information we are now in a position to show how the micro-, meso-, and macro-pore volumes change with conversion (Fig. 8), with the microporous volume fraction decreasing, the mesoporous volume fraction increasing, and the macroporous fraction remaining constant. These variations have implications on how the internal surfaces participate in the chemical reaction, which will be a subject of a subsequent paper.

4. CONCLUDING COMMENTS

Pore size distributions have been obtained for single particle using gas adsorption for micropores, the observed constancy of the macropores and a volume balance for the mesopores. The ability of the electrodynamic balance to measure densities of single macroporous particles, without need to differentiate as in conventional liquid displacement methods between macropores and interparticle interstices, provides a ready way for obtaining the mesoporous regime. The results can be depicted graphically as pie charts as shown for three conversions in Fig. 9.

The study provides support for the hypothesis of Hurt et al. (1988) that densification of the microporous regions is due to pore elimination. The interesting finding is the increase in the mesoporous region with increasing conversion, suggesting a crucial role for the mesopores in the reaction.

REFERENCES

- Bar-ziv E., Jones D. B., Spjut R. E., Dudek D. R., Sarofim, A. F. and Longwell, J.P. (1989). Comb & Flame, 75, 81, 1989
- Bellezza, C. (1985). Naples, Dept. of Chem. Eng. Dissertation.
- D'Amore M., Dudek, D.R., Sarofim, A.F., and Longwell J.P. (1988). Powder Tech., 56, 129.
- Davis E.J. and Ray, A.K.(1980). J. Colloid Interface Sci. 75, 566.
- Dollimore, D. and Heal, G.L. (1970). J. Colloid Interfaces Sci. 33, 508
- Dubinin, M.M. (1966) in Chemistry and Physics of Carbon (ed. by P. L. Walker) Vol. 2, p. 86, Marcel Drekker, New York
- Dubinin, M.M. and Astakhov, V.A. (1971). Adv. Chem. Ser. 102, 69
- Dudek, D.R. (1988). Mass. Inst, of Tech. PhD Thesis
- Dudek, E.R., Longwell, J.P. and Sarofim, A.F. (1988) Energy & Fuels, 3, 24.
- Gan, H., Nandi, S.P. and Walker, P.L., Jr. (1972). Fuel. 51, 272
- Gavalas, G.R. (1980). AIChE. 26, 577
- Hurt, R.H., Dudek, E.R., Sarofim, A.F. and Longwell, J.P. (1988). Carbon, 26, 433,
- Kerstein, A.R., and Niksa, S. (1985). Twentieth Symp. (Int.) on

Comb. The Combustion Institute, Pittsburgh, Pa. p. 941
- Lamond, T. and Marsh H. (1964). Carbon. 1, 281
- Marsh, H., Iley, M., Berger, J. and Siemieniewska (1975). Carbon, 13, 103
- Medek, J. (1977). Fuel. 56, 131
- Mohanty, K.K., Ottino, J.M. and Davis, H.T. (1982). Chem. Engng. Sci. 37, 905
- Philip, M.A. (1981). Mass.Inst. of Technology, M.S. Thesis
- Rand, B.J. (1974). J. Colloid Interface Sci. 48, 183
- Reyes, S. and Jensen, K.F. (1986). Chem. Engng. Sci. 41, 333
- Smith, I.W. (1982). Nineteenth Symp. (Int.) on Comb. The Combustion Institute, Pittsburgh, Pa. p. 1045
- Spitzer, Z., Biba, V. and Kadlec, O. (1976). 14, 151
- Spjut, R.E. (1985). Mass. Inst. of Tech. Ph.D. Thesis
- Spjut, R.E., Sarofim, A.F., and Longwell, J.P. (1985). Langmuir, 1, 355.
- Waters, B.J., Squires, R.G., and Laurendeau, N.M. (1988b). Comb. Sci and Tech. 62, 187
- Wuerker, R.F., Shelton, H., and Langmuir, R.V. (1959) J. Appl. Phys., 30, No 3, 342.

LIST OF SYMBOLS

A	differential molar work of adsorption, cal mol^{-1}
E	characteristics free energy of adsorption, cal mol^{-1}
R	gas constant, 1.987 cal mol^{-1}
T	particle temperature, K
V	particle volume, cm_3
V_0	initial particle volume, cm_3
W	single particle meso- plus macropore volume per unit initial mass, $cm^3\ g^{-1}$
W_0	single particle initial meso- plus macropore volume per unit mass, $cm^3\ g^{-1}$
c	parameter in BET equation
f	fractional conversion
h	parameter in Dubinin equation
k	interaction constant in eq.(4). For CO_2 $k=7.51\ 10^2$ cal nm^{-3} $mole^{-1}$.
p	adsorption gas pressure, atm
p_s	adsorption gas saturation pressure, atm
r_e	pore radius, nm
s	amount of gas adsorbed at relative pressure p/p_s, $mol\ g^{-1}$
s_m	amount of gas adsorbed in a complete monolayer, $mol\ g^{-1}$
s_{ts}	amount of gas adsorbed in the total micropore volume, $mol\ g^{-1}$
w	micropore volume per unit particle mass filled at pressure p/p_s, $cm^3\ g^{-1}$
w_{ts}	total micropore volume per unit particle mass, $cm^3\ g^{-1}$
ϵ	single particle porosity
θ	degree of filling of micropores
ρ	apparent particle density, $g_3 cm^{-3}$
ρ_t	true particle density, g cm^{-3}
Σ	particle shrinkage factor

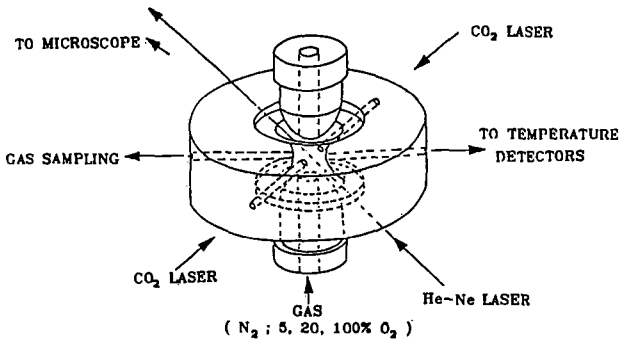

Fig. 1 - The Electrodynamic Thermogravimetric Analyser

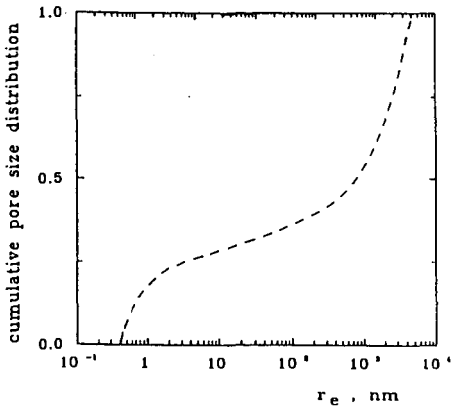

Fig. 2

Cumulative pore size distribution on volume basis

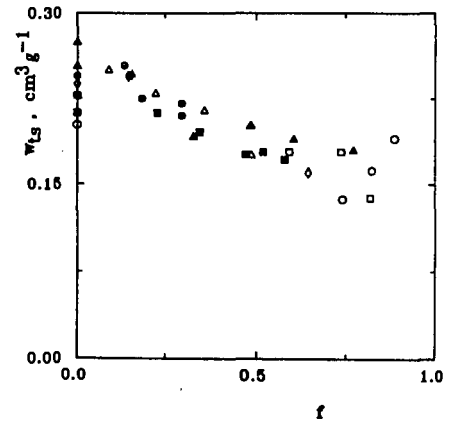

Fig. 3

Eight separate aingle particle "Spherocarb" oxidations in EDTGA.
Micropores volume per unit particle mass as a function of conversion.

◇ ▲ △ ○ □ 100% O_2
● ◒ 21% O_2
■ 100% CO_2

▨ 100,000 "Spherocarb" particles oxidation with 21% O_2 in CTGA.

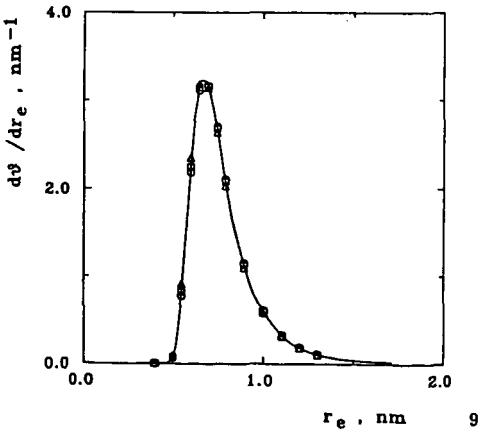

Fig. 4

Single particle "Spherocarb" oxidation with 21% O_2 in EDTGA.
Micropores size distribution at various conversions.

△ f = 0.14
□ 0.23
○ 0.52
solid line unreacted char

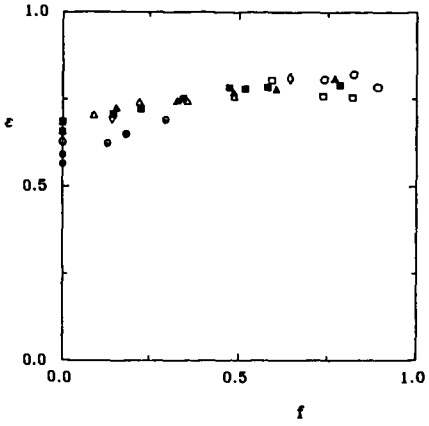

Fig. 5

Eight separate single particle "Spherocarb" oxidations in EDTGA.
Particle porosity as a function of conversion.
◇▲△○□ 100% O_2
●◒ 21% O_2
■ 100% CO_2

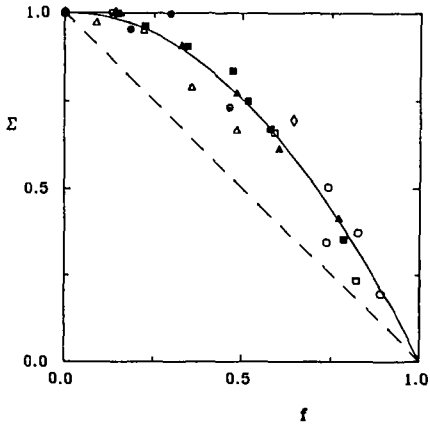

Fig. 6

Eight separate single particle "Spherocarb" oxidations in EDTGA.
Particle shrinkage factor as a function of conversion.
◇▲△○□ 100% O_2
●◒ 21% O_2
■ 100% CO_2
dashed line shrinking core model
solid line best fit line

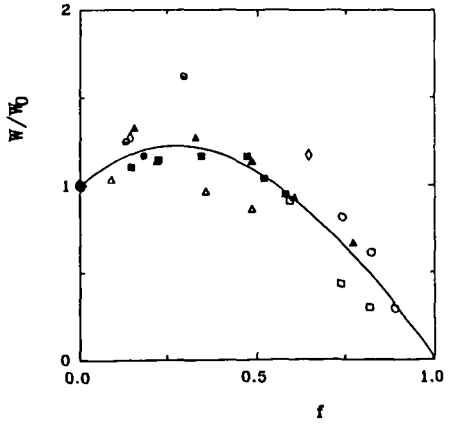

Fig. 7

Eight separate single particle "Spherocarb" oxidations in EDB.
Particle meso- plus macropore volume per unit initial mass, normalized in respect to the value at f=0, as a function of conversion.
◇▲△○□ 100% O_2
●◒ 21% O_2
■ 100% CO_2
solid line best fit line

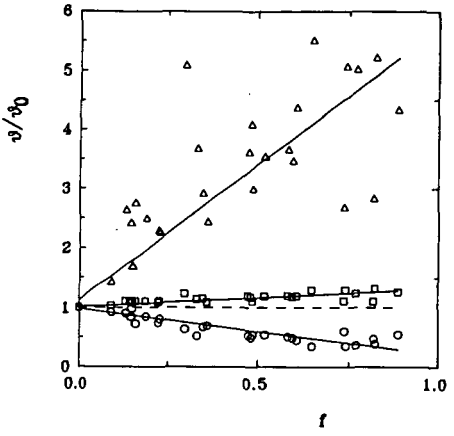

Fig. 8 - Eight separate single particle "Spherocarb" oxidations in EDB.
Pores volume fractions, normalized with respect to the value at f=0, as a function of conversion.

□ total pores volume fraction
--- macropores
△ mesopores
○ micropores

Fig. 9 - Single particle "Spherocarb" oxidation in EDB.
Volume fraction of porea and carbon at various conversions.